

Uncertainty estimation for time series forecasting via Gaussian process regression surrogates

Leonid Erlygin
Skoltech
Moscow, Russia
MIPT
Moscow, Russia
erlygin.la@phystech.edu

Vladimir Zholobov
Skoltech
Moscow, Russia
MIPT
Moscow, Russia

Valeriia Baklanova
Sber
Moscow, Russia
HSE
Moscow, Russia

Evgeny Sokolovskiy
Sber
Moscow, Russia

Alexey Zaytsev
BIMSA
Beijing, China
Skoltech
Moscow, Russia

ABSTRACT

Machine learning models are widely used to solve real-world problems in science and industry. To build robust models, we should quantify the uncertainty of the model’s predictions on new data. This study proposes a new method for uncertainty estimation based on the surrogate Gaussian process model. Our method can equip any base model with an accurate uncertainty estimate produced by a separate surrogate. Compared to other approaches, the estimate remains computationally effective with training only one additional model and doesn’t rely on data-specific assumptions. The only requirement is the availability of the base model as a black box, which is typical. Experiments for challenging time-series forecasting data show that surrogate model-based methods provide more accurate confidence intervals than bootstrap-based methods in both medium and small-data regimes and different families of base models, including linear regression, ARIMA, and gradient boosting.

CCS CONCEPTS

• **Computing methodologies** → **Machine learning**; *Artificial intelligence*.

KEYWORDS

uncertainty estimation, surrogate models, time-series, Gaussian processes, bootstrap

ACM Reference Format:

Leonid Erlygin, Vladimir Zholobov, Valeriia Baklanova, Evgeny Sokolovskiy, and Alexey Zaytsev. 2023. Uncertainty estimation for time series forecasting via Gaussian process regression surrogates. In *KDD ’23: SIGKDD conference*

Permission to make digital or hard copies of all or part of this work for personal or classroom use is granted without fee provided that copies are not made or distributed for profit or commercial advantage and that copies bear this notice and the full citation on the first page. Copyrights for components of this work owned by others than ACM must be honored. Abstracting with credit is permitted. To copy otherwise, or republish, to post on servers or to redistribute to lists, requires prior specific permission and/or a fee. Request permissions from [permissions@acm.org](https://permissions.acm.org).

KDD ’23, August 06–10, 2023, SIGKDD, USA

© 2023 Association for Computing Machinery.

ACM ISBN 978-1-4503-XXXX-X/18/06...\$15.00

<https://doi.org/XXXXXXXX.XXXXXXX>

Table 1: Mean ranks on Forecasting data benchmark problems for four UE approaches with respect to the Miscalibration area metric. We consider three types of black box models: ordinary linear regression (OLS), ARIMA and implementation of Gradient Boosting CatBoost equipped with intrinsic uncertainty estimates. Best results are highlighted with bold font, second best results are underscored.

| UE method \ Base model | OLS | ARIMA | CatBoost | Mean |
|------------------------|--------------|--------------|--------------|--------------|
| Base model | 3.062 | 2.83 | 3.435 | 3.109 |
| Best Bootstrap | 2.825 | 1.734 | 2.826 | 2.462 |
| Naive Surrogate | <u>2.25</u> | 3.064 | 1.793 | <u>2.369</u> |
| Our Surrogate | 1.862 | <u>2.372</u> | <u>1.946</u> | 2.06 |

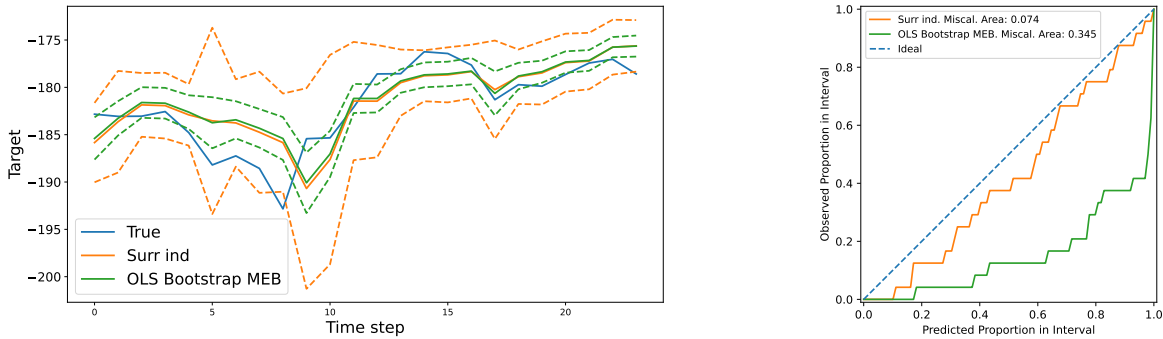
on knowledge discovery and data mining. ACM, New York, NY, USA, 13 pages.
<https://doi.org/XXXXXXXX.XXXXXXX>

1 INTRODUCTION

Ability to estimate the uncertainty of the model’s predictions is a long-standing problem in machine learning, which has high practical value. It is particularly important in risk-sensitive areas such as medical machine learning [19] and object detection in autonomous driving [9].

Among other applications, uncertainty estimation is desirable in time series forecasting. The problem is crucial for both classic [23] and deep learning models as well [25, 55]. For application examples you can look at share price prediction tasks [11]: it is important to detect when macroeconomic change occurs, and new data starts to come from a different distribution. Accurately estimated confidence intervals could help to detect such changes: confidence intervals are wide on out-of-distribution data, thus, one should retrain a regression model using new data.

We consider uncertainty estimation for a fixed pre-trained deterministic regression model, which we will call the *base model* throughout the paper. For most experiments, we consider the time series forecasting problem, but we rarely pay attention the specifics



(a) Uncertainty estimation for our method Surr ind. and the best bootstrap method OLS Bootstrap MEB for one-step-ahead time series forecasting problem. The left plot shows obtained predictions and corresponding uncertainty estimates, the right plot provides insight on the quality of the uncertainty estimation. The description of dataset A is available below.

Figure 1: Example of uncertainty estimation with our method and other methods: the left plot shows obtained predictions and corresponding uncertainty estimates, the right plot provides insight on the quality of the uncertainty estimation. The description of dataset A is available below.

of the data at hand. We assume that the base model accurately predicts target value, but lacks an uncertainty estimation for its predictions. We want to equip it with the ability to efficiently estimate point confidence intervals or uncertainty estimates for predictions. While, the most natural approach is a variant of bootstrap it faces two challenges that are hard to handle without looking into a particular problem: dependencies in sequential time series data and inefficiency of bootstrap that requires training of multiple models and using all of them during inference. The former problem can be mitigated via taking the dependency structure into the account, while you need to make correct assumptions about the dependence structure [23]. The later problem can be mitigated with e.g. MCMC dropout approach [24], but this approximation reduces the quality of uncertainty estimation [41].

The alternative proposed in this paper is to train a *surrogate* model on the same input data used to train the base model. If the problem requires representation learning, we can train a surrogate model that takes embeddings as an input or in other way approach deep kernel learning [51]. A similar approach was used to provide uncertainty estimates for image classification problems [27]. Their Gaussian process classifier was trained on top of hidden image representations computed by CNN. We also select Gaussian process regression as a functional class for the surrogate model training, as it provides reliable uncertainty estimates [20] and straightforward to train [50].

After a surrogate model is trained, we construct a combined model, which uses a base model to make target value prediction and a surrogate model to estimate uncertainty for the prediction of base model. To make uncertainty estimation reliable, we design a loss function that allows the surrogate model to imitate the base model predictions, while keeping the method computationally efficient

and avoiding contamination of the training sample with points we are uncertain about.

We compare the proposed method for uncertainty estimation with bootstrap ensemble methods and other relevant methods [40]. Our evidence include the experiments with different base models: linear models, ARIMAs, gradient boostings [7]. Most of these methods have their own intrinsic ways for uncertainty estimation, see e.g. [42] for ARIMA, [8, 30] for gradient boosting. The experiments show that produced uncertainty estimates with our surrogate approach is more accurate than predictions from even build-in methods designed specifically for these models. In this paper, we focus on time-series forecasting problem, as one of the most challenging and requiring close attention to the structure of the dependence of the data with a convenient tools for the comparison of performance over diverse regression problems. An example of our uncertainty estimation is in Figure 1 demonstrates that the surrogate uncertainty estimates don't suffer from overconfidence typical for other methods. Moreover, Table 1 shows that this evidence is not anecdotal, it holds for wide range of datasets and types of base models: our approach to construction of a surrogate model outperforms basic uncertainty estimates for consider classes of models, the best bootstrap-based approach we found and naive training of a surrogate uncertainty estimation.

Our claims are the following:

- The proposed surrogate uncertainty estimation for a black box model is natural and easy to implement. The corresponding loss function encapsulates primal requirements to uncertainty estimators, while keeping the pipeline simple.
- Additional computational costs during training and inference are small. We prove this for the used Gaussian process regression surrogate.

- For time series forecasting problem, the quality of surrogate uncertainty estimates is better than the performance of model-specific approaches and bootstrap approaches that take into account structure of the data. This observation holds for different base black boxes that require uncertainty estimation.

We conduct experiments for the time series forecasting problem, while we don't use any specific properties of this problem. It is likely, that similar results hold for a more general class of regression problems, while we don't provide evidence in this paper.

2 RELATED WORK

Uncertainty types. The uncertainty of a value is understood as its characteristic, which describes a certain allowable spread of its values and arises due to the inaccuracy of measuring instruments, the inconsistency of the allowed restrictions with the real data and the processes behind them, as well as with the approximations contained in the model itself. There are three types of uncertainty in the machine learning literature: aleatoric uncertainty, epistemic uncertainty and combined type [39].

Aleatoric uncertainty [1] is related to the probabilistic nature of the data and the impossibility of overcoming it. The simplest example is an error in the data received by a measuring device with a given error. We may say that such a scatter occurs by chance and may not be eliminated. On the other hand, we may determine its characteristics using, for example, methods for building a model with inhomogeneous heteroscedastic noise.

Epistemic uncertainty [1] is related to the limitations of the model used for forecasting. It arises due to the inaccuracy of the approximations embedded in the model or as a result of applying the model to new data that differ from those used in its construction. Such uncertainty may be reduced, for example, by improving the model or by using a more correct data set to train it.

Ensemble approach for uncertainty quantification. One of the approaches to obtain estimates of uncertainty is the construction of an ensemble of similar, but different in some nuances, models. At the same time, to obtain estimates of uncertainty, the spread of different model predictions is considered [24, 29]. For example, an estimate of the forecast variance at a point may be its empirical estimate from the forecast vector of an ensemble of models.

The most well-known approach of constructing an ensemble of models — using of bootstrap [40]. During bootstrapping, objects for training are sampled from the training set with repetitions. The resulting sample is used to train models from ensembles. With a reasonable choice of the number of models in the ensemble, this method allows one to obtain fairly accurate statistical estimates of the data.

However, such a procedure, in its basic form, considers data as a set of independent objects. Here we consider sequential data in which there is a temporal connection. There are sampling methods that extend the basic version of the bootstrap, designed specifically for working with time series and sequential data models. In particular, a block bootstrap [22, 35, 36] or auto-regressive data sampling [23] is used.

Recent work considers obtaining uncertainty estimates using ensembles of deep models [24]. Due to the significant number of

parameters available in neural networks, the slightest changes in the initialization of the model before the training lead to changes in the trained model. Moreover, estimates of the mean and scatter for each predicted point may be obtained. However, for classical machine learning models with a small number of parameters applied to a small amount of data, this approach is poorly applicable since it is more difficult to achieve a variety of outputs.

Gaussian process approach for Uncertainty Quantification. Sometimes there is a situation when the test set has a different distribution than the train set. This problem is known as the out-of-distribution (OOD) problem. Therefore, a model is needed that can detect this and give a uniform distribution to classes.

The Gaussian Process Regression (GPR) [50] model has this property. It works well even in the case of misspecified model [54]. It is a well-known fact that the GPR model was introduced as a fully probabilistic substitute for the multilayer perceptron (MLP). That idea was pointed out in the observation [33], where a GPR is an MLP with infinite units in the hidden layer. Traditional GPR models have been extended to more expressive variants, for example, to Deep Gaussian Process [5].

There are quite a lot of studies of GPR properties. For instance, it is a case where we have the misspecified problem statement [45] for GPR. In [54], they obtain the exact expression for interpolation error in the misspecified case for stationary Gaussian process, using an infinite grid designs of experiments. This setup is correct due to it does not significantly affect the results [53].

In addition, there are some applied examples where GPR is considered. For example, it is problems with time-series forecasting [38]. Specifically, the article [14] shows that GPR can be applied for time-series forecasting even for large data scenario. In this case, there is adopted so-called sparse Gaussian process regression for e.g. multiple-step ahead forecasting.

However, there are some issues in the high-dimensional problems: it is crucial to extract features or reduce dimension. To solve this problem, there was proposed a simple solution [28], using spectral normalization to the weights in each layer [32].

Surrogates models. The use of an ensemble of models is justified from a theoretical point of view, but there are limitations that do not allow it to be fully applied as a universal way of estimating uncertainty. It is the ambiguity of solving the problem of choosing a sampling procedure for constructing an ensemble of models. Moreover, that type of method is computationally expensive: it is necessary to build a large number of models, which is not always possible for both machine models and less computationally efficient deep learning models.

Therefore, an alternative approach based on surrogate modelling is used. A surrogate model or meta-model $\tilde{f}(x)$ is created for a model $\hat{f}(x)$. Due to the procedure for constructing such a model, we assume $\tilde{f}(x) \approx \hat{f}(x)$ [31].

Due to the adequacy of the quality of the model and the estimation of uncertainty, it seems natural to use regression based on Gaussian processes as a surrogate model for the original one. A similar approach was used to improve active learning [44].

3 METHODS

In this section, we pose a formal uncertainty estimation problem in Section 3.1 and introduce our methods in Section 3.2. For the sake of comparison we provide ideas of bootstrap approaches in Section 3.5.

3.1 Problem formulation

Let us have training dataset $\mathcal{D} = \{(\mathbf{x}_i, y_i)\}_{i=1}^N$, where \mathbf{x}_i is an input data sample from the domain $\mathcal{X} \subset \mathbb{R}^d$, and y_i is a corresponding target from the domain $\mathcal{Y} \subset \mathbb{R}$. We assume that the training dataset was sampled from a joint distribution of inputs and targets $p(\mathbf{x}, y)$. We also make standard Bayesian assumptions for the data generation process: first parameters $\theta \in \Theta$ of some random function $f_\theta : \mathcal{X} \rightarrow \mathcal{Y}$ are sampled, then y is sampled from the conditional distribution $p(y|\mathbf{x}, \theta)$. For a regression problem, this conditional distribution is usually assumed to be Gaussian: $p(y|\mathbf{x}, \theta) = \mathcal{N}(y; f_\theta(\mathbf{x}), \sigma_\theta^2(\mathbf{x}))$.

With these assumptions predictive distribution can be written as:

$$p(y|\mathbf{x}, \mathcal{D}) = \int_{\Theta} p(y|\mathbf{x}, \theta) p(\theta|\mathcal{D}) d\theta \quad (1)$$

where $p(y|\mathbf{x}, \theta)$ - target likelihood given parameters of function f_θ and input point \mathbf{x} , $p(\theta|\mathcal{D})$ - posterior distribution of parameters θ .

In practice, the predictive distribution is rarely tractable, so many methods use point estimates: $p(y|\mathbf{x}, \mathcal{D}) \approx p(y|\mathbf{x}, \theta)$, where θ can be e.g. a maximum likelihood estimate, substituting $p(\theta|\mathcal{D})$ with a delta-function. In this case, we treat the mean value of this distribution $\hat{f}(\mathbf{x})$ as the prediction of the model.

We can formulate our problem in two ways. The first goal is an accurate estimation of the variance $\hat{\sigma}^2(\mathbf{x})$ of the distribution $p(y|\mathbf{x}, \mathcal{D})$ at a point \mathbf{x} quantifying the uncertainty about the model prediction. The second goal is estimation of the shortest confidence interval of the significance level α such that the true value fall into this interval with probability α , and the interval is the shortest among all such intervals. If $p(y|\mathbf{x}, \theta)$ is Gaussian, two formulations coincide, as the confidence interval for the prediction with probability α can be written as

$$CI_\alpha = [\hat{f}(\mathbf{x}) - z_{\alpha/2} \hat{\sigma}(\mathbf{x}), \hat{f}(\mathbf{x}) + z_{\alpha/2} \hat{\sigma}(\mathbf{x})], \quad (2)$$

where $z_{\alpha/2}$ is the $\alpha/2$ quantile of standard normal distribution.

If we have a probabilistic model, these problems admit reasonable solutions. However, in many cases we have only a black-box deterministic *base* model $\hat{f}(\mathbf{x})$. So, our final goal is to equip a deterministic regression model with uncertainty estimation.

In the following sections, we propose a surrogate modelling approach, which can be used to estimate the uncertainty of a deterministic base model. Later, we separately discuss an ensemble-based model.

3.2 Surrogate based on Gaussian process regression

We present a universal and numerical efficient approach that requires no assumptions about the model and can equip any black-box model with an uncertainty estimate. Given a deterministic *base* model $\hat{f}(\mathbf{x})$, we introduce another *surrogate* model $\tilde{f}(\mathbf{x})$. We select

$\tilde{f}(\mathbf{x})$ such that it directly models the target distribution $p(y|\mathbf{x}, \mathcal{D})$ while mimicking the black-box model predictions from $\hat{f}(\mathbf{x})$.

A natural choice for such a probabilistic model is the Gaussian process regression (GPR) [50] as it produces the Gaussian distribution $p(y|\mathbf{x}, \theta)$.

Intuitively, the surrogate model trained on the same dataset approximates base model $\tilde{f} \approx \hat{f}$, which itself approximates underlying distribution $\hat{f}(\mathbf{x}) \approx \mathbb{E}_{p(y|\mathbf{x}, \mathcal{D})} y$ and thus we expect it to have adequate uncertainty estimates.

We note, that if the input dimension is sufficiently low, we can train GP using the initial input data. If the data modality requires representation learning, we use embeddings from the base model to train Gaussian process with deep representation-based kernel.

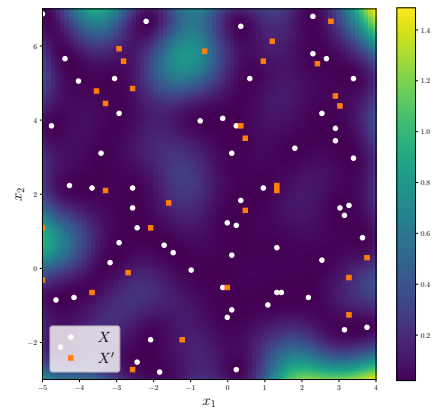


Figure 2: Example of Uncertainty estimation for two dimensional input via a matching surrogate model. The variance estimate corresponds to the fill color at the point. At points from the initial training sample X the uncertainty is almost zero, while for points from the additional sample X' it takes reasonable values reflecting our absence of knowledge about the true function values at these locations.

3.3 Matching surrogate model training

Using the approach described above as it is to obtain a surrogate model is naive, as we expect that if the training sample is the same, then the trained model would be the same in cases of the base model and a surrogate model. Numerous pieces of evidence suggest that this is not true, and we can get different models, even if we use the same dataset and the same class of models.

On the other hand, the base model is available as a black box, so one can query it at the points of interest, improving the surrogate model by showing it more relevant training data. For Gaussian process regression, we can use this information efficiently. Moreover, the uncertainty estimate will have a natural kernel-style behaviour: the uncertainty increases as we go away from the points from the initial sample used to train the base model.

We assume that the surrogate model $\tilde{f}(\mathbf{x})$ is a realization of Gaussian process. More precisely, $\tilde{f}(\mathbf{x}) \sim GP(0, k(\mathbf{x}, \mathbf{x}')|\mathcal{D})$ for a

covariance function $k(\mathbf{x}, \mathbf{x}')$ from a parametric family, zero mean and condition on available data \mathcal{D} . The conditional mean $m(\mathbf{x})$ and variance $\sigma^2(\mathbf{x})$ given the sample of observations \mathcal{D} at a new point \mathbf{x} in this case have the following form:

$$\begin{aligned} m(\mathbf{x}) &= \mathbf{k}^T K^{-1} \mathbf{y} = \mathbf{k}^T \boldsymbol{\alpha}, \quad \boldsymbol{\alpha} = K^{-1} \mathbf{y}, \\ \sigma^2(\mathbf{x}) &= k(\mathbf{x}, \mathbf{x}) - \mathbf{k}^T K^{-1} \mathbf{k}, \end{aligned}$$

where $\mathbf{k} = \{k(\mathbf{x}, \mathbf{x}_i)\}_{i=1}^N$, $K = \{k(\mathbf{x}_i, \mathbf{x}_j)\}_{i,j=1}^N$. To find the parameters of covariance function, one maximizes the likelihood of the data given the covariance function. In our case, we have an additional requirement to match the base model $\hat{f}(\mathbf{x})$. So, the loss function is the sum of two loss terms:

$$L(\tilde{f}, \hat{f}, \mathcal{D}, \mathcal{D}'_{\tilde{f}}) = -(1 - C) \log p(\mathbf{y} | X, \tilde{f}) + C \sum_{i=1}^L (\tilde{f}(\mathbf{x}'_i) - \hat{f}(\mathbf{x}'_i))^2, \quad (3)$$

where $\log p(\mathbf{y} | X, \tilde{f})$ is the data likelihood, $C \in [0, 1]$ is the second term weight coefficient. The second term is the sum of squared difference between the surrogate model prediction $\tilde{f}(\mathbf{x}'_i)$ and the base model $\hat{f}(\mathbf{x}'_i)$ for a sample $\mathcal{D}'_{\tilde{f}} = \{(\mathbf{x}_i, \hat{f}(\mathbf{x}'_i))\}_{i=1}^L$. In our experiments, inputs in $\mathcal{D}'_{\tilde{f}}$ are selected uniformly randomly over the domain of interest. The pseudo-code for the proposed method that we name *Surr Ind* in pytorch style is available in Appendix B.

In the terminology of sparse Gaussian process regression, points from \mathcal{D} are *inducing* points, as we condition our distribution on them. We use additional points from $\mathcal{D}'_{\tilde{f}}$ only to adjust the model parameters. So, we (1) keep the computational complexity low and (2) uncertainty estimation growing if we go away from the initial training sample.

Let us put these two statements formally.

LEMMA 3.1. *The computational complexity for the evaluation of the loss function (3) equals to $O(N^3) + O(LN)$.*

PROOF. Using the formula for the likelihood for Gaussian process regression, we get

$$\begin{aligned} L(\tilde{f}, \hat{f}, \mathcal{D}, \mathcal{D}') &= \frac{(1-C)}{2} \left(N \log \pi + \log \det |K| + \mathbf{y}^T \boldsymbol{\alpha} \right) + \\ &+ C \left(K_{X'X} \boldsymbol{\alpha} - \hat{f}(X') \right)^T \left(K_{X'X} \boldsymbol{\alpha} - \hat{f}(X') \right), \end{aligned}$$

where $K_{X'X} = \{k(\mathbf{x}'_i, \mathbf{x}'_j)\}_{i,j=1}^{L,N}$, $\hat{f}(X') = \{\hat{f}(\mathbf{x}'_1), \dots, \hat{f}(\mathbf{x}'_L)\}$.

So, we need to evaluate two terms: the likelihood and the squared loss. To calculate the likelihood we need $O(N^3)$, as we need the inverse and the determinant of the covariance matrix of size $N \times N$. Note, that if we have the inverse, we calculate $\boldsymbol{\alpha} = K^{-1} \mathbf{y}$ in $O(N^2)$. So, to get the predictions we need $O(LN)$ additional operations in addition. Summing both complexities, we obtain the desired $O(N^3) + O(LN)$. \square

So, as long as we keep L of order of magnitude similar to N , we have little additional computational power required. Moreover, we can afford L to be of order N^2 , which is impossible with the naive baselines above.

The second statement about amount of the noise available is also natural. If we move \mathbf{x} to infinity, then $\sigma^2(\mathbf{x})$ tends to $k(\mathbf{x}, \mathbf{x})$

for any reasonable covariance function, whatever $\mathcal{D}'_{\tilde{f}}$ were used, as the components of the covariance vector $k(\mathbf{x}, \mathbf{x}')$ goes to zero. An example of application of our approach is presented in Figure 2.

Surrogate-model-aware inference. After the surrogate model is trained, we use the following combined model: the point target values predictions come from base model $\hat{f}(\mathbf{x})$, and the variance $\hat{\sigma}^2(\mathbf{x})$ from the surrogate model. We assume, that the distribution of the output is Gaussian, and can use the formula (2) to produce confidence intervals, if required. The added computational complexity of our approach during inference is the evaluation cost for the surrogate model variance.

3.4 Baseline surrogate model training

We can also consider other design of experiments for training the surrogate model \tilde{f} without changing the log-likelihood loss function, but changing the data we use for training. Let us consider four natural options:

- (1) (Surr I) $\mathcal{D} = \{(\mathbf{x}_i, y_i)\}_{i=1}^N$
- (2) (Surr II) $\mathcal{D}_{\tilde{f}} = \{(\mathbf{x}_i, \hat{f}(\mathbf{x}_i))\}_{i=1}^N$
- (3) (Surr III) $\mathcal{D}_{\tilde{f}} \cup \mathcal{D}'_{\tilde{f}} = \{(\mathbf{x}_i, \hat{f}(\mathbf{x}_i))\}_{i=1}^N \cup \{(\mathbf{x}'_i, \hat{f}(\mathbf{x}'_i))\}_{i=1}^L$
- (4) (Surr IV) $\mathcal{D} \cup \mathcal{D}'_{\tilde{f}} = \{(\mathbf{x}_i, y_i)\}_{i=1}^N \cup \{(\mathbf{x}'_i, \hat{f}(\mathbf{x}'_i))\}_{i=1}^L$

The first dataset is the original training dataset. In the second case, we approximate the base model directly, while we can lost information about aleatoric uncertainty presented in the initial dataset. In the third and the fourth case, we append additional points from input domain \mathcal{X} to the training dataset, to better approximate the base model. In fourth case we use initial targets on original dataset. These options are natural baselines with strong empirical evidence behind them.

In experiments with dataset types (2), (3) and (4) we add variances at each point for each target $\hat{f}(\mathbf{x}_i)$, corresponding to inaccuracy for the base model predictions. For points from \mathcal{D} we use a small noise variance values. For points from new datasets we use a single following value:

$$\hat{\sigma}^2 = \frac{1}{N} \sum_{i=1}^N \left((\hat{f}(\mathbf{x}_i) - y_i) - \mu_{\sigma} \right)^2, \quad \mu_{\sigma} = \frac{1}{N} \sum_{i=1}^N (\hat{f}(\mathbf{x}_i) - y_i)$$

This variance is assigned for each point, as we can pass noise variances for each point as an input during training for almost all popular realizations of GPR.

3.5 Bootstrap-based ensemble methods

In this section, we briefly describe bootstrap or Monte-Carlo approach to uncertainty estimation for time series. If we can sample from $p(\boldsymbol{\theta} | \mathcal{D})$, then using a sample $\boldsymbol{\theta}_i$ from this distribution, Monte-Carlo approximation holds:

$$p(y | \mathbf{x}, \mathcal{D}) \approx \frac{1}{k} \sum_{i=1}^k p(y | \mathbf{x}, \boldsymbol{\theta}_i).$$

Following this direction, we get an estimate of the variance as

$$\hat{\sigma}^2(\mathbf{x}) = \frac{1}{k-1} \sum_{i=1}^k (\hat{f}_{\boldsymbol{\theta}_i}(\mathbf{x}) - \bar{f}(\mathbf{x}))^2,$$

where $\tilde{f}(\mathbf{x}) = \frac{1}{k} \sum_{i=1}^k \hat{f}_i(\mathbf{x})$.

The problem is that we can't sample from the distribution $p(\theta|\mathcal{D})$ to get an independent sample of θ_i . The bootstrap algorithm proposes a variant of such sampling. The pairs (\mathbf{x}_i, y_i) from the training sample \mathcal{D} come from an unknown distribution F whose parameters we want to estimate. From this sample, we form k subsamples \mathcal{D}_i of size N with replacement. The most general option involves the simultaneous sampling of pairs of data vectors and features (\mathbf{x}_i, y_i) . Moreover, some observations (\mathbf{x}_i, y_i) in the j -th subsample may be repeated or absent. An alternative solution is to sample the data and feature vectors separately, for example, for the j -th subsample, mix the order y_j with a fixed matrix X . Anyway, using a resulting set \mathcal{D}_i we train a model $\hat{f}_i(\mathbf{x}) = f_{\theta_i}(\mathbf{x})$. Consolidating all models, we obtain an ensemble of size k .

The bootstrap procedure requires training k independent models, which is inefficient. Another challenge is a difference between the bootstrap distribution of parameters and the true posterior distribution $p(\theta|\mathcal{D})$. In practice, the problem is even more severe for time series forecasting. Several appropriate bootstrap procedures for time series try to take this issue into account. In this work, we will use three additional types of time-series bootstraps to cover the most broadly used approaches. They are Maximum Entropy-based bootstrap (MEB), Stationary Block Bootstrap (SBB), and Bootstrapping Stationary Autoregressive processes (BSAP). Let us briefly describe them and their assumptions.

SBB belongs to the family of block methods given in [21, 35, 36]. The main idea is to split a sequence to blocks and permute these block during each bootstrap iteration. If the time series is stationary, we have provable good properties of the procedure. By adding stochasticity in the splitting procedure, we ensure, that SBB mimics the true posterior distribution.

BSAP originates from [23]. For this approach, the assumption must be fulfilled that the series is stationary and generated by an autoregressive (AR) model.

$$y_i = \beta_1 y_{i-1} + \dots + \beta_p y_{i-p} + \varepsilon_i, i \in \mathbb{Z}.$$

The main idea is to fit AR model and get its parameters $(\hat{\beta}_1, \dots, \hat{\beta}_p)^\top$. After it, we obtain residuals $\tilde{\varepsilon}_i$

$$\tilde{\varepsilon}_i = y_i - \hat{\beta}_1 y_{i-1} - \dots - \hat{\beta}_p y_{i-p} - \frac{1}{n-p} \sum_{k=p+1}^n \hat{\varepsilon}_k, i = p+1, \dots, n.$$

Afterwards we equally likely sample $n-p-1$ points from the set $\{\tilde{\varepsilon}_{p+1}, \dots, \tilde{\varepsilon}_n\}$ with repetitions. Then using it get new points via AR model with sample noises.

$$y_i^* = \hat{\beta}_1 y_{i-1}^* + \dots + \hat{\beta}_p y_{i-p}^* + \varepsilon_i^*, i \in \mathbb{Z}. \quad (4)$$

As most of the time-series are non-stationary, we use Holt-Winters transformation [52] to get stationary time series before the application of BSAP.

Maximum Entropy-based bootstrap [47] follows a different idea. We sort all target values and remember the indexes for these targets from the original sample. Then, we sample values from this interval, round them, so each of the sample value correspond to the closest one from the training sample, then we use the indexes used for sorting to get a replacement for each value. For this approach, the ergodic theorem [46] is satisfied, which guarantees that the

bootstrap values will be close to the values of the sample: it is more likely that points close to the points from the sample will appear. Because of this, the resulting subsamples will differ from the sample itself, but not much. So we get a new set of samples and models for the ensemble and will be able to estimate the uncertainty.

4 EXPERIMENTS

We structure the experiments section in the following way. Subsection 4.1 presents the used time series forecasting benchmark. Subsection 4.2 introduced used quality metrics. Then we describe the main comparison of our approach with others for different types of base models. Subsection on ablation study concludes this section. Not all experiments made to the main text of the paper, so for more detailed experiments we refer an interesting leader to Appendix C. In all tables below best results are highlighted with **bold** font, second best results are underscored.

4.1 Datasets

Time series forecasting data FD benchmark. One of the largest benchmarks for predicting one-dimensional time series is the Monash time series forecasting archive (TSForecasting) [13]. It contains 26 publicly available time series datasets from different applied domains with equal and variable lengths. The goal for each dataset is time series forecasting for a specific time horizon h . The data cover nine diverse areas: tourism, banking, Internet, energy, transport, economy, sales, health and nature.

Some sets repeat in slightly different versions: the frequency of the time series considered in them changes (day, month, quarter or year), or missing values are included and excluded. Because of this, the total number of sample options reaches 50.

We chose TSForecasting for the variety of presented sequential data, which allows us to cover a large class of tasks. In most cases, one sample contains a fairly large number of time series, 2600 on average. There are also six additional very long time series, two of which have a length of more than 7 million.

Original paper [13] provides a more detailed description of each dataset. All the metadata for building the model (prediction horizon, context length, periodicity, etc.) follow the settings from this project. For some datasets in [13], there was no metadata. We excluded such datasets from consideration. Therefore, the number of datasets has decreased to 19 datasets with one-dimensional data and one dataset with single multi-dimensional time series. From each dataset with one-dimensional data first two time series were taken.

For one-dimensional time series from TSForecasting with target values only, we use p lags as features. For example, i -th point its label y and features \mathbf{x} are

$$y = y_i, \quad \mathbf{x} = (y_{i-1}, \dots, y_{i-p}).$$

For multi-dimensional time series, we use provided features.

We split time series into train and test data using test data with the size of $(h+p)$ for one-dimensional time series and h for multi-dimensional time series. Moreover, to speed up computations, only time series of length $\max(2 \cdot lag, 200)$ are used.

Financial data. As concrete applied examples, we consider two datasets for the time series prediction connected to the financial industry. We can't disclose the names of the targets and name them

Dataset A and Dataset B. The target values are modified to hide their true value and scale, while these changes don't affect the obtained metrics.

Both datasets have clear out-of-distribution parts related to the changes caused by COVID-19 and other crises, so they can be used to evaluate the uncertainty estimation for time series. Moreover, they have another challenge related to the small number of points available for training.

4.2 Evaluation metrics

To provide a multi-faceted evaluation, the results include values of various quality metrics for the uncertainty quantification. We present values of the Root Mean Square Calibration Error (RMSCE) and miscalibration area in the main text. Better calibrated models have larger RMSCE and smaller miscalibration area. Additional metrics and related discussion are presented in appendix section A.

Here we use critical difference (CD) diagrams to compare statistically methods. Following the recommendation in [6] we used Friedman test [10] to reject the null hypothesis. Afterwards we consider the pairwise post-hoc analysis where the average rank comparison is replaced by a Wilcoxon signed-rank test with Holm's alpha (5%) correction[15]. The results are visualized by a critical difference diagram proposed in [6]. In the diagram a thick horizontal line shows a group of models (a clique) that are not-significantly different in terms of metric value. We use framework to build CD diagram from the article [16]. There are CD diagrams for regression metric (RMSE) and calibration metric (Miscalibration Area).

4.3 Considered uncertainty estimates

The complexity of uncertainty estimation problem lead to diverse solutions specific to different approaches. Our question is how we can overcome the intrinsic and model-agnostic methods for different classes of base models. We consider ordinary least squares (OLS), CatBoost (a realization of Gradient boosting equipped with uncertainty estimate) and ARIMA. For all methods the hyperparameters are default.

For all base models we consider different ways to construct uncertainty estimates. We start with build-in approaches for each base model. OLS and ARIMA models obtain uncertainty estimates based on a Bayesian assumption about the model parameters. Gradient boosting model uses auxiliary models that minimize the quantile loss.

We compare the built-in approaches with alternatives that uses the base model as a black box or can train it in case of bootstraps. Considered bootstraps include Naive bootstrap (Naive BS) and advanced bootstrap types (MEB BS, SBB BS, BSAP BS), described in the relevant section above. In ablation study, we also compare our approach *Surr Ind* (surrogate model with initial training points as inducing) with different types of surrogate models (Surr I, Surr II, Surr III and Surr IV).

Additional details on used procedure to construct baseline surrogate models are presented in Appendix, Section C.4.

4.4 Main results

Our goal here is compare different methods with the focus on the quality of uncertainty estimates. The main results for Forecasting

Table 2: Ranks of regression and uncertainty estimation metrics aggregated over Forecasting data benchmark

| Uncertainty estimate | Base model | RMSE | Miscal. Area | RMSCE | ENCE |
|----------------------|------------|--------------|--------------|--------------|--------------|
| Built-in | | <u>3.825</u> | 4.075 | 4.075 | 4.075 |
| Naive BS | | 4.438 | 3.988 | 4.112 | 3.975 |
| MEB BS | | 4.95 | 4.912 | 4.95 | 5.025 |
| SBB BS | OLS | 4.088 | 5.412 | 5.312 | 5.488 |
| BSAP BS | | 3.05 | 4.075 | 4.1 | 5.012 |
| Surr I | | <u>3.825</u> | <u>2.962</u> | <u>2.862</u> | <u>2.438</u> |
| Surr Ind | | <u>3.825</u> | 2.575 | 2.588 | 1.988 |
| Built-in | | 4.957 | 4.717 | 4.739 | 4.087 |
| Naive BS | | 2.0 | <u>3.054</u> | <u>3.022</u> | 3.489 |
| MEB BS | | 3.804 | 4.043 | 4.076 | 3.793 |
| SBB BS | ARIMA | 4.87 | 4.413 | 4.457 | 3.848 |
| BSAP BS | | <u>2.196</u> | 2.728 | 2.728 | <u>3.522</u> |
| Surr I | | 5.087 | 5.098 | 5.054 | 5.522 |
| Surr Ind | | 5.087 | 3.946 | 3.924 | 3.739 |
| Built-in | | <u>3.978</u> | 5.178 | 5.133 | 3.6 |
| Naive BS | | 3.989 | 4.344 | 4.389 | 4.844 |
| MEB BS | | 4.733 | 4.5 | 4.489 | 4.889 |
| SBB BS | CatBoost | 4.2 | 5.411 | 5.389 | 6.311 |
| BSAP BS | | 3.144 | 3.811 | 3.911 | 4.378 |
| Surr I | | <u>3.978</u> | 2.256 | 2.178 | <u>2.0</u> |
| Surr Ind | | <u>3.978</u> | <u>2.5</u> | <u>2.511</u> | 1.978 |

data are in Table 2 . Since Forecasting data has a lot of time series, we decided to count ranks and average it for all pairs of a base model and corresponding uncertainty estimate for it. Even higher level aggregation is provided in the teaser table 1 with Our surrogate being a pen name for Surr Ind and Best bootstrap being a pen name for BSAP BS. We note, that at both low level and high rank-based level comparison in almost all cases our Surr Ind provides the best results. Surr I is also a strong baseline, which make them a sound alternative in some cases.

Another insights are provided by critical difference diagrams [6] and plot them in Figures 3, 5. More detailed comparison with discussion of obtained critical difference diagrams are given in Appendix, Section C.2.

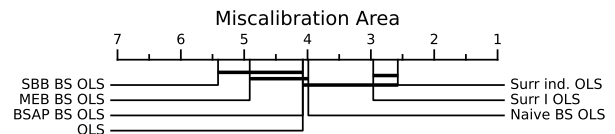


Figure 3: OLS base model comparison of Miscalibration area on Forecasting data

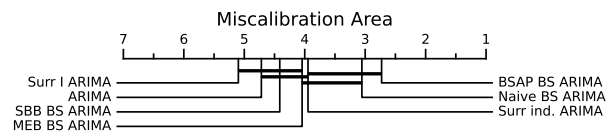


Figure 4: ARIMA base model comparison of RMSE on Forecasting data

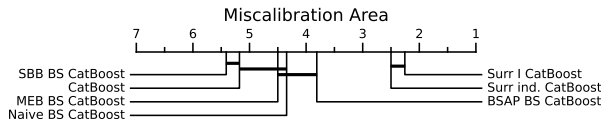


Figure 5: OLS base model comparison of RMSE on Forecasting data

We also provide metrics for separate datasets A and B to give a taste, what is not only the rank, but also related differences in metrics. Tables 3 and 4 provides detailed uncertainty estimation quality metrics for Dataset A and Dataset B respectively. Again, our Surr Ind provides superior uncertainty estimation metrics in many cases.

So, the presented results show that Surr Ind and Surr I outperform other methods and are non-significantly different from each other. In addition, some bootstrap methods are non-significantly different from each other.

4.5 Comparison of surrogate models

There are various strategies for training surrogate models in addition to our main line. In particular, we compare our approach with four Baseline types of surrogate: Surr I – trained on the initial dataset \mathcal{D} , Surr II trained on \mathcal{D}_f , Surr III trained on $D_f \cup D'_f$ and Surr IV trained on $D \cup D'_f$. In our experiments $|D'_f| = 20$ and noise assumed in targets for Surr II, Surr III, Surr IV with variance computed by formula (3.4).

Results on Forecasting Data are presented in Table 5; critical difference diagram for OLS base model is in Figure 8. Surr Ind outperforms the basic approach without additional points Surr I as well as other approaches with slightly worse results for CatBoost base model.

4.6 Selection of hyperparameters for Surr Ind

C and L selection. Our approach has two main hyperparameters: the weight of the second term in the loss function C and the number of additional points in the sample \mathcal{D}'_f . In this subsection, we investigate, how they affect the performance of our models. We fix one hyperparameters and vary another producing the quality metric miscalibration area for each particular pair. We present results for one dataset A, results for other datasets are similar. The results of the experiments are in Figures 6. We see, that we observe higher metrics for moderate values of C and high number of generated points L comparable to the initial sample size N . On other hand, we see, that after some moment the performance halts to improve. Thus, we recommend to use C in the interval $[0.5, 1]$ and $L \approx N$.

Choice of kernel for surrogate model. Here we investigate which kernel is preferable for GPR surrogate model. We train Surr Ind with linear and with RBF kernels and measure their uncertainty estimation quality on Forecasting Data. In Figure 7 Miscalibration Area of RBF and linear kernel is compared, with different base models. One can see, that linear kernel performs slightly better with all base models, and particularly with OLS. Moreover, linear kernel-based surrogate model have better rank, computed on Forecasting

Table 3: Quality metrics for regression and uncertainty estimation on Dataset A

| Uncertainty estimate | Base model | RMSE | Miscal. Area | RMSCE | ENCE |
|----------------------|------------|------------------|--------------|--------------|--------------|
| Built-in | | 16362.093 | 0.167 | 0.184 | 0.824 |
| Naive BS | | 16696.277 | 0.204 | 0.229 | 1.189 |
| MEB BS | | 16512.081 | 0.32 | 0.358 | 2.213 |
| SBB BS | OLS | 17394.776 | <u>0.054</u> | <u>0.067</u> | 0.476 |
| BSAP BS | | 20228.613 | 0.242 | 0.276 | 2.596 |
| Surr I | | 16362.093 | 0.028 | 0.036 | 0.234 |
| Surr Ind | | 16362.093 | 0.084 | 0.098 | <u>0.384</u> |
| Built-in | | 25524.539 | 0.269 | 0.313 | 0.689 |
| Naive BS | | 16296.585 | <u>0.144</u> | <u>0.16</u> | 0.61 |
| MEB BS | | 26411.274 | 0.45 | 0.513 | 4.075 |
| SBB BS | ARIMA | 32248.943 | 0.43 | 0.479 | 2.078 |
| BSAP BS | | <u>23403.858</u> | 0.099 | 0.115 | <u>0.612</u> |
| Surr I | | 25524.539 | 0.292 | 0.33 | 0.823 |
| Surr Ind | | 25524.539 | 0.358 | 0.4 | 1.317 |
| Built-in | | 33352.452 | 0.489 | 0.563 | 0.987 |
| Naive BS | | <u>31155.193</u> | 0.456 | 0.535 | 14.201 |
| MEB BS | | 31949.12 | 0.466 | 0.538 | 9.144 |
| SBB BS | CatBoost | 33602.92 | 0.495 | 0.57 | 22.932 |
| BSAP BS | | 30253.746 | 0.469 | 0.54 | 13.866 |
| Surr I | | 33352.452 | 0.354 | 0.394 | <u>1.374</u> |
| Surr Ind | | 33352.452 | <u>0.373</u> | <u>0.413</u> | 1.437 |

Table 4: Quality metrics for regression and uncertainty estimation on Dataset B

| Uncertainty estimate | Base model | RMSE | Miscal. Area | RMSCE | ENCE |
|----------------------|------------|--------------|--------------|--------------|--------------|
| Built-in | | 0.028 | 0.35 | 0.384 | 1.801 |
| Naive BS | | 0.029 | 0.363 | 0.406 | 2.922 |
| MEB BS | | 0.028 | 0.408 | 0.452 | 2.507 |
| SBB BS | OLS | 0.028 | 0.363 | 0.399 | 1.913 |
| BSAP BS | | 0.03 | 0.314 | 0.352 | 2.12 |
| Surr I | | 0.028 | <u>0.058</u> | <u>0.067</u> | <u>0.416</u> |
| Surr Ind | | 0.028 | 0.054 | 0.063 | 0.348 |
| Built-in | | 0.063 | 0.374 | 0.435 | 0.836 |
| Naive BS | | 0.029 | 0.41 | 0.451 | 2.647 |
| MEB BS | | 0.039 | 0.272 | 0.295 | 1.057 |
| SBB BS | ARIMA | 0.065 | 0.085 | 0.094 | 0.465 |
| BSAP BS | | <u>0.035</u> | 0.206 | 0.245 | 1.177 |
| Surr I | | 0.063 | 0.37 | 0.407 | 1.561 |
| Surr Ind | | 0.063 | <u>0.086</u> | <u>0.101</u> | 0.342 |
| Built-in | | 0.029 | 0.455 | 0.535 | 2250.228 |
| Naive BS | | <u>0.028</u> | 0.225 | 0.263 | 3.336 |
| MEB BS | | 0.03 | 0.29 | 0.345 | 2.417 |
| SBB BS | CatBoost | 0.031 | 0.334 | 0.386 | 4.092 |
| BSAP BS | | 0.026 | 0.178 | 0.215 | 1.934 |
| Surr I | | 0.029 | 0.046 | 0.055 | 0.479 |
| Surr Ind | | 0.029 | 0.045 | 0.055 | <u>0.486</u> |

Data, than RBF kernel-based one. So, we select linear kernel for Surr Ind approach in the main study.

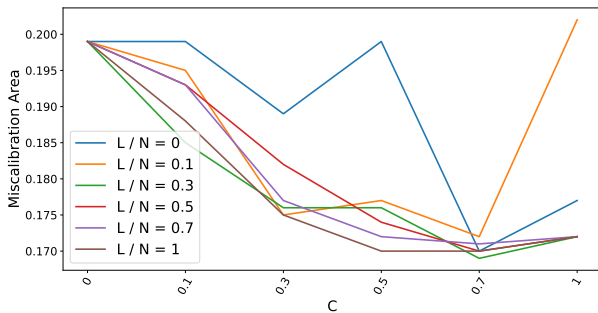
5 DISCUSSION AND CONCLUSIONS

We have shown that the surrogate-model-based approach produces accurate confidence interval predictions for different base models on different datasets. Calibration and regression metrics of surrogate models are comparable with classical bootstrap ensemble methods and in most cases are better. This means that we can get accurate uncertainty estimates without the necessity to train many models using bootstrap and select a proper bootstrap technique among existing ones.

The computational complexity of our method coincides with that of Gaussian process regression for the available training sample. From one point of view, it is a con, especially for a complex base

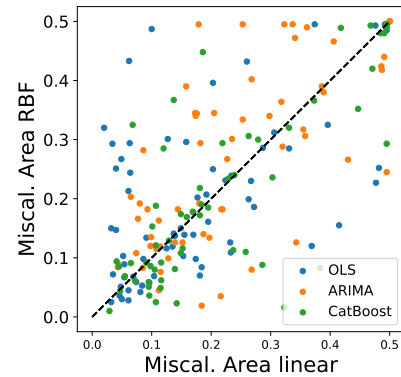
Table 5: Ranks of uncertainty estimation metrics for surrogate model type of uncertainty estimation aggregated over Forecasting data benchmark

| Uncertainty estimate | Base model | Miscal. Area | RMSCE | ENCE |
|----------------------|------------|--------------|--------------|--------------|
| Built-in | OLS | 4.28 | 4.31 | 4.74 |
| Surr I | | <u>2.73</u> | <u>2.66</u> | <u>2.75</u> |
| Surr II | | 3.94 | 3.93 | 4.0 |
| Surr III | | 4.31 | 4.37 | 4.12 |
| Surr IV | | 3.55 | 3.56 | 3.06 |
| Surr Ind | | 2.19 | 2.17 | 2.33 |
| Built-in | ARIMA | 3.669 | 3.653 | 3.898 |
| Surr I | | 3.975 | 3.924 | 4.636 |
| Surr II | | <u>3.314</u> | <u>3.229</u> | 3.246 |
| Surr III | | 3.551 | 3.559 | 3.271 |
| Surr IV | | 3.602 | 3.678 | <u>3.068</u> |
| Surr Ind | | 2.89 | 2.958 | 2.881 |
| Built-in | CatBoost | 4.681 | 4.655 | 3.966 |
| Surr I | | 2.655 | 2.629 | <u>2.586</u> |
| Surr II | | 3.5 | 3.509 | 3.845 |
| Surr III | | 3.94 | 3.94 | 4.526 |
| Surr IV | | 3.362 | 3.388 | 3.526 |
| Surr Ind | | <u>2.862</u> | <u>2.879</u> | 2.552 |


Figure 6: Dependence of the surrogate uncertainty estimate quality metric Miscalibration area on the hyperparameter C for different number of generated points

model. Moreover, as most time series data have moderate sample sizes, it is not a burden. From the other point of view, $O(N^3)$ can be prohibitive in some cases. We suggest using sparse Gaussian process regression (GPR) [37] or other large-data-set variants of GPR widely available in modern literature [26] and used in industrial problems [3]. We would highlight the importance of selection of the set of inducing points in our approach, as they are the points with zero model uncertainty in them, and can be selected with this thought in mind. Detailed investigation on how to select a proper method or a proper set of inducing points to condition Gaussian process regression is an interesting question for future research.

We also limited ourselves to the time series forecasting problem. For time series forecasting, we have a ready benchmark with datasets of moderate size, which allows numerous experiments and consideration of diverse base models. Moreover, Gaussian process regression works well in estimation uncertainty for multiple-step


Figure 7: Miscalibration Area of Surr ind. with linear kernel vs Surr ind. with RBF kernel over Datasets A, B and Forecasting data

ahead forecast [12], making them even more plausible. Other benchmarks like UCI [2] would also help to understand the performance of the surrogate GPR better, with our work being a good starting point.

Another possible application include yet-unsolved problem of the estimation of uncertainty for deep learning. It arises in NLP problems [41], open-set face recognition [17], OOD detection in computer vision [1]. We provide an example, that our method works for the state-of-the-art neural network for time series forecasting InceptionTime. Combining our ideas with large scale GP and deep kernel learning [34, 51], we should be able to fill this gap better.

Last but not the least is the limitations of GP models in terms of types of modelled uncertainty. We would say, that taking into account uncertainty of the parameters estimation for Gaussian process regression can help in some problems, see [48] for relevant ideas.

To sum up, we believe that the presented work would help practitioners to construct uncertainty estimates for their models using a Gaussian process regression surrogate trained in the manner suggested in the paper. Some questions related to the presented method remain open, while the excessive wisdom of the crowd makes them primarily engineering, while attractive and worth exploring.

ACKNOWLEDGMENTS

We thank Evgenya Romanenkova for helpful advices and thorough paper reading.

REFERENCES

- [1] Moloud Abdar, Farhad Pourpanah, Sadiq Hussain, Dana Rezazadegan, Li Liu, Mohammad Ghavamzadeh, Paul Fieguth, Xiaochun Cao, Abbas Khosravi, U Rajendra Acharya, et al. 2021. A review of uncertainty quantification in deep learning: Techniques, applications and challenges. *Information Fusion* 76 (2021), 243–297.
- [2] Stephen D Bay, Dennis Kibler, Michael J Pazzani, and Padhraic Smyth. 2000. The UCI KDD archive of large data sets for data mining research and experimentation. *ACM SIGKDD explorations newsletter* 2, 2 (2000), 81–85.
- [3] EV Burnaev and AA Zaytsev. 2015. Surrogate modeling of multifidelity data for large samples. *Journal of Communications Technology and Electronics* 60 (2015), 1348–1355.
- [4] Youngseog Chung, Ian Char, Han Guo, Jeff Schneider, and Willie Neiswanger. 2021. Uncertainty toolbox: an open-source library for assessing, visualizing,

- and improving uncertainty quantification. *arXiv preprint arXiv:2109.10254* 2109 (2021), 1–8.
- [5] Andreas Damianou and Neil D Lawrence. 2013. Deep Gaussian processes. In *Artificial intelligence and statistics*. PMLR, JMLR Workshop and Conference Proceedings, Scottsdale, AZ, USA, 207–215.
 - [6] Janez Demšar. 2006. Statistical comparisons of classifiers over multiple data sets. *The Journal of Machine Learning Research* 7 (2006), 1–30.
 - [7] Anna Veronika Dorogush, Vasily Ershov, and Andrey Gulin. 2018. CatBoost: gradient boosting with categorical features support. *arXiv preprint arXiv:1810.11363* (2018).
 - [8] Tony Duan, Avati Anand, Daisy Yi Ding, Khanh K Thai, Sanjay Basu, Andrew Ng, and Alejandro Schuler. 2020. Ngboost: Natural gradient boosting for probabilistic prediction. In *International Conference on Machine Learning*. PMLR, 2690–2700.
 - [9] Di Feng, Ali Harakeh, Steven L. Waslander, and Klaus Dietmayer. 2022. A Review and Comparative Study on Probabilistic Object Detection in Autonomous Driving. *IEEE Transactions on Intelligent Transportation Systems* 23, 8 (2022), 9961–9980. <https://doi.org/10.1109/ITITS.2021.3096854>
 - [10] Milton Friedman. 1940. A comparison of alternative tests of significance for the problem of m rankings. *The Annals of Mathematical Statistics* 11, 1 (1940), 86–92.
 - [11] Yugo Fujimoto, Kei Nakagawa, Kentaro Imajo, and Kentaro Minami. 2022. Uncertainty Aware Trader-Company Method: Interpretable Stock Price Prediction Capturing Uncertainty. *arXiv:arXiv:2210.17030*
 - [12] Agathe Girard, Carl Rasmussen, Joaquin Q Candela, and Roderick Murray-Smith. 2002. Gaussian process priors with uncertain inputs application to multiple-step ahead time series forecasting. *Advances in neural information processing systems* 15 (2002).
 - [13] Rakshitha Godahewa, Christoph Bergmeir, Geoffrey I Webb, Rob J Hyndman, and Pablo Montero-Manso. 2021. Monash time series forecasting archive. *arXiv preprint arXiv:2105.06643* (2021).
 - [14] Tobias Gutjahr, Holger Ulmer, and Christoph Ament. 2012. Sparse Gaussian processes with uncertain inputs for multi-step ahead prediction. *IFAC Proceedings Volumes* 45, 16 (2012), 107–112.
 - [15] Sture Holm. 1979. A simple sequentially rejective multiple test procedure. *Scandinavian journal of statistics* (1979), 65–70.
 - [16] Hassan Ismail Fawaz, Germain Forestier, Jonathan Weber, Lhassane Idoumghar, and Pierre-Alain Muller. 2019. Deep learning for time series classification: a review. *Data Mining and Knowledge Discovery* 33, 4 (2019), 917–963.
 - [17] Roman Kail, Kirill Fedyanin, Nikita Muravev, Alexey Zaytsev, and Maxim Panov. 2022. ScaleFace: Uncertainty-aware Deep Metric Learning. *arXiv preprint arXiv:2209.01880* (2022).
 - [18] Harshavardhan Kamarthi, Ling kai Gong, Alexander Rodriguez, Chao Zhang, and B Aditya Prakash. 2021. When in doubt: Neural non-parametric uncertainty quantification for epidemic forecasting. *Advances in Neural Information Processing Systems* 34 (2021), 19796–19807.
 - [19] Benjamin Kompa, Jasper Snoek, and Andrew L. Beam. 2021. Second opinion needed: communicating uncertainty in medical machine learning. *npj Digital Medicine* 4, 1 (05 Jan 2021), 4. <https://doi.org/10.1038/s41746-020-00367-3>
 - [20] Slawomir Koziel and Leifur Leifsson. 2013. *Surrogate-based modeling and optimization*. Springer.
 - [21] Hans R Kunsch. 1989. The jackknife and the bootstrap for general stationary observations. *The Annals of Statistics* 17, 3 (1989), 1217–1241.
 - [22] Hans R. Kunsch. 1989. The Jackknife and the Bootstrap for General Stationary Observations. *The Annals of Statistics* 17, 3 (1989), 1217 – 1241. <https://doi.org/10.1214/aos/117634265>
 - [23] SK Lahiri and SN Lahiri. 2003. *Resampling methods for dependent data*. Springer Science & Business Media, New York.
 - [24] Balaji Lakshminarayanan, Alexander Pritzel, and Charles Blundell. 2017. Simple and scalable predictive uncertainty estimation using deep ensembles. *Advances in neural information processing systems* 30 (2017).
 - [25] Bryan Lim and Stefan Zohren. 2021. Time-series forecasting with deep learning: a survey. *Philosophical Transactions of the Royal Society A* 379, 2194 (2021), 20200209.
 - [26] Haitao Liu, Yew-Soon Ong, Xiaobo Shen, and Jianfei Cai. 2020. When Gaussian process meets big data: A review of scalable GPs. *IEEE transactions on neural networks and learning systems* 31, 11 (2020), 4405–4423.
 - [27] Jeremiah Liu, Zi Lin, Shreyas Padhy, Dustin Tran, Tania Bedrax Weiss, and Balaji Lakshminarayanan. 2020. Simple and Principled Uncertainty Estimation with Deterministic Deep Learning via Distance Awareness. In *Advances in Neural Information Processing Systems*, H. Larochelle, M. Ranzato, R. Hadsell, M.F. Balcan, and H. Lin (Eds.), Vol. 33. Curran Associates, Inc., Virtual, 7498–7512. <https://proceedings.neurips.cc/paper/2020/file/543e83748234f7cbab21aa0ade66565f-Paper.pdf>
 - [28] Jeremiah Liu, Zi Lin, Shreyas Padhy, Dustin Tran, Tania Bedrax Weiss, and Balaji Lakshminarayanan. 2020. Simple and principled uncertainty estimation with deterministic deep learning via distance awareness. *Advances in Neural Information Processing Systems* 33 (2020), 7498–7512.
 - [29] Jeremiah Liu, John Paisley, Marianthi-Anna Kioumourtzoglou, and Brent Coll. 2019. Accurate uncertainty estimation and decomposition in ensemble learning. *Advances in Neural Information Processing Systems* 32 (2019).
 - [30] Andrey Malinin, Liudmila Prokhorenkova, and Aleksei Ustimenko. 2020. Uncertainty in gradient boosting via ensembles. *arXiv preprint arXiv:2006.10562* (2020).
 - [31] Lu Mi, Hao Wang, Yonglong Tian, Hao He, and Nir N Shavit. 2022. Training-free uncertainty estimation for dense regression: Sensitivity as a surrogate. In *Proceedings of the AAAI Conference on Artificial Intelligence*, Vol. 36. AAAI Press, Palo Alto, California USA, 10042–10050.
 - [32] Takeru Miyato, Toshiki Kataoka, Masanori Koyama, and Yuichi Yoshida. 2018. Spectral Normalization for Generative Adversarial Networks. In *International Conference on Learning Representations*. ICLR, Vancouver Convention Center, Vancouver Canada, 1–26.
 - [33] Radford M Neal. 2012. *Bayesian learning for neural networks*. Vol. 118. Springer Science & Business Media, New York.
 - [34] Sebastian W Ober, Carl E Rasmussen, and Mark van der Wilk. 2021. The promises and pitfalls of deep kernel learning. In *Uncertainty in Artificial Intelligence*. PMLR, 1206–1216.
 - [35] Efsthathios Paparoditis and Dimitris N. Politis. 2001. Tapered Block Bootstrap. *Biometrika* 88, 4 (2001), 1105–1119. <http://www.jstor.org/stable/2673704>
 - [36] Dimitris N. Politis and Joseph P. Romano. 1994. The Stationary Bootstrap. *J. Amer. Statist. Assoc.* 89, 428 (1994), 1303–1313. <http://www.jstor.org/stable/2290993>
 - [37] Joaquin Quinero-Candela and Carl Edward Rasmussen. 2005. A unifying view of sparse approximate Gaussian process regression. *The Journal of Machine Learning Research* 6 (2005), 1939–1959.
 - [38] Stephen Roberts, Michael Osborne, Mark Ebdon, Steven Reece, Neale Gibson, and Suzanne Aigrain. 2013. Gaussian processes for time-series modelling. *Philosophical Transactions of the Royal Society A: Mathematical, Physical and Engineering Sciences* 371, 1984 (2013), 20110550.
 - [39] Christopher J Roy and William L Oberkampf. 2011. A comprehensive framework for verification, validation, and uncertainty quantification in scientific computing. *Computer methods in applied mechanics and engineering* 200, 25-28 (2011), 2131–2144.
 - [40] Jun Shao. 1996. Bootstrap model selection. *Journal of the American statistical Association* 91, 434 (1996), 655–665.
 - [41] Artem Shelmanov, Evgenii Tsybmalov, Dmitri Puzyrev, Kirill Fedyanin, Alexander Panchenko, and Maxim Panov. 2021. How Certain is Your Transformer?. In *Proceedings of the 16th Conference of the European Chapter of the Association for Computational Linguistics: Main Volume*. 1833–1840.
 - [42] Ralph D Snyder, J Keith Ord, and Anne B Koehler. 2001. Prediction intervals for ARIMA models. *Journal of Business & Economic Statistics* 19, 2 (2001), 217–225.
 - [43] Kevin Tran, Willie Neiswanger, Junwoong Yoon, Qingyang Zhang, Eric Xing, and Zachary W Ulissi. 2020. Methods for comparing uncertainty quantifications for material property predictions. *Machine Learning: Science and Technology* 1, 2 (2020), 025006.
 - [44] Evgenii Tsybmalov, Sergei Makarychev, Alexander Shapeev, and Maxim Panov. 2019. Deeper Connections between Neural Networks and Gaussian Processes Speed-up Active Learning. In *Proceedings of the 28th International Joint Conference on Artificial Intelligence (IJCAI'19)*. AAAI Press, Macao, China, 3599–3605.
 - [45] Aad Van Der Vaart and Harry Van Zanten. 2011. Information Rates of Nonparametric Gaussian Process Methods. *Journal of Machine Learning Research* 12, 6 (2011).
 - [46] Hrishikesh D Vinod. 2006. Maximum entropy ensembles for time series inference in economics. *Journal of Asian Economics* 17, 6 (2006), 955–978.
 - [47] Hrishikesh D Vinod and Javier López-de Lacalle. 2009. Maximum entropy bootstrap for time series: the meboot R package. *Journal of Statistical Software* 29 (2009), 1–19.
 - [48] Johan Wagberg, Dave Zachariah, Thomas Schon, and Petre Stoica. 2017. Prediction performance after learning in Gaussian process regression. In *Artificial Intelligence and Statistics*. PMLR, 1264–1272.
 - [49] Bin Wang, Tianrui Li, Zheng Yan, Guangquan Zhang, and Jie Lu. 2020. DeepPIPE: A distribution-free uncertainty quantification approach for time series forecasting. *Neurocomputing* 397 (2020), 11–19.
 - [50] Christopher K.I. Williams and Carl Edward Rasmussen. 2006. *Gaussian processes for machine learning*. Vol. 2. MIT press, Cambridge, MA.
 - [51] Andrew Gordon Wilson, Zhiting Hu, Ruslan Salakhutdinov, and Eric P Xing. 2016. Deep kernel learning. In *Artificial intelligence and statistics*. PMLR, 370–378.
 - [52] Peter R Winters. 1960. Forecasting sales by exponentially weighted moving averages. *Management science* 6, 3 (1960), 324–342.
 - [53] Alexey Zaytsev and Evgeny Burnaev. 2017. Minimax approach to variable fidelity data interpolation. In *Artificial Intelligence and Statistics*. PMLR, 652–661.
 - [54] Alexey Zaytsev, Evgenya Romanenkova, and Dmitry Ermilov. 2018. Interpolation error of Gaussian process regression for misspecified case. In *Conformal and Probabilistic Prediction and Applications*. PMLR, 83–95.
 - [55] Lingxue Zhu and Nikolay Laptev. 2017. Deep and confident prediction for time series at Uber. In *2017 IEEE International Conference on Data Mining Workshops (ICDMW)*. IEEE, 103–110.

A DETAILS ON THE QUALITY METRICS FOR UNCERTAINTY QUANTIFICATION

First of all, there is the most common metric in uncertainty estimation papers, the calibration curve [4, 18, 49]. The calibration curve displays the true frequency of points in each interval versus the predicted proportion of points in that interval. It may be constructed by comparing the observed distribution of points in the intervals $(-\infty, x] \forall x \in (-\infty, \infty)$ with predicted distributions. Thus, "well-calibrated" models have residuals whose standard deviations are close to the predicted standard deviations of the model. Based on the calibration curve we calculate the miscalibration area.

As stated above, a perfectly calibrated model will have normalized residuals that are Gaussian, giving a diagonal calibration line. Therefore, the quality of the models may be quantified by the proximity of their calibration curves to this ideal diagonal curve. Miscalibration area — the area of the set representing the difference between the calibration curve and the triangle formed by the diagonal, horizontal lower and vertical right lines for a unit square. Smaller values correspond to a more accurate calibration [43].

A close metric is the Root Mean Square Calibration Error (RM-SCE):

$$\sqrt{\frac{1}{n} \sum_{j=1}^n (p_j - \hat{p}_j)^2}, \quad (5)$$

where \hat{p}_j — the predicted probability of falling into the confidence interval given by some quantile, p_j — the percentage of test sample points that fall within the interval.

The calibration metrics presented above, in some cases, fail to distinguish between informative and non-informative uncertainty forecasts. To solve this problem we present two additional metrics for estimating model calibration, ENCE and the coefficient of variation of the predicted standard deviations.

Let σ_t be the standard deviation of the prediction for the t -th object. Choose a parameter n — the number of bins, such that the sample size $N = nb$. Therefore, $\{B_j\}_{j=1}^N$ such that the sets of indices $B_j = \{(j-1)\frac{N}{n} + 1, \dots, j \cdot \frac{N}{n}\}$.

Auxiliary metrics may be calculated for true values y_t for each bin, objective function predictions \hat{y}_t and predictions variance $\hat{\sigma}_t^2$. Root Mean-Variance:

$$RMV_j = \sqrt{\frac{1}{|B_j|} \sum_{t \in B_j} \hat{\sigma}_t^2} \quad (6)$$

Root Mean Square Error:

$$RMSE_j = \sqrt{\frac{1}{|B_j|} \sum_{t \in B_j} (y_t - \hat{y}_t)^2} \quad (7)$$

As a result, ENCE is calculated:

$$ENCE = \frac{1}{N} \sum_{j=1}^N \frac{|RMV_j - RMSE_j|}{RMV_j} \quad (8)$$

Another important metric is the coefficient of variation c_u :

$$c_u = \frac{\sqrt{\frac{\sum_{t=1}^T (\hat{\sigma}_t - \mu_\sigma)^2}{T-1}}}{\mu_\sigma}, \quad (9)$$

where $\mu_\sigma = \frac{1}{N} \sum_{i=1}^N \hat{\sigma}_i$ is average standard deviation. Low values indicate a narrow variance of uncertainty estimates, which may indicate poor quality of predictions on the validation set.

The last metric we consider is Prediction Interval Coverage Probability (PICP) [49]. PICP is defined as the proportion of true values that are within the confidence interval of the prediction. The higher this figure, the better. However, using only it is not enough as we may achieve 100% of the given metric value (all prediction intervals will cover the true value) by setting the prediction interval to infinity.

B SURR IND PSEUDOCODE

Below we provide pseudocode for our Surr Ind approach.

```
# sample new points uniformly
X_new = np.random.uniform(
    low=np.min(x_history_norm),
    high=np.max(x_history_norm),
    size=(L, num_features),
)

# Find optimal model hyperparameters
gpr_model.train()
gpr_likelihood.train()
optimizer = Adam(gpr_model.parameters())
mll = ExactMarginalLogLikelihood(
    gpr_likelihood, gpr_model
)

for i in range(training_iter):
    optimizer.zero_grad()

    output = gpr_model(x_history_norm)

    # Calc log likelihood loss
    loss_mll = -mll(output, y_history_norm)

    # Calc mse loss

    # get base model predictions
    base_model_pred = get_base_model_pred()
    # go to gpr inference mode
    # and compute posterior mean
    gpr_model.inference()
    gpr_model_pred = gpr_model(X_new).mean
    gpr_model.train()

    loss_mse = F.mse_loss(
        gpr_model_pred,
        base_model_pred)

    # aggregate loss
    loss = (1 - C) * loss_mll + C * loss_mse
    loss.backward()
    optimizer.step()
```

C ADDITIONAL EXPERIMENTS

C.1 Quality of uncertainty estimation for different base models

The results of the base models are given in Table 6 for Dataset A and in Table 7 for Dataset B. We present both regression quality and quality of uncertainty estimation. For all considered forecasting horizons Gaussian process regression (GPR) approach is in top two for both considered uncertainty estimation quality metrics. Consequently, it is a good candidate for a surrogate-based uncertainty estimate, if we can make GPR close to a base model.

Table 6: Regression and calibration metrics for base models on Dataset A. Best results are highlighted with bold font, second best results are underscored

| Model | Horizon | RMSE | RMSCE | Miscal. Area | ENCE |
|----------|---------|------------------|--------------|--------------|--------------|
| GPR | 3 | 14712.701 | 0.319 | 0.262 | 0.322 |
| OLS | | <u>11933.3</u> | 0.57 | 0.495 | 3.285 |
| CatBoost | | 14173.191 | 0.57 | 0.495 | 0.999 |
| ARIMA | | 9035.37 | <u>0.333</u> | <u>0.286</u> | <u>0.695</u> |
| GPR | 6 | 12725.005 | 0.199 | 0.164 | 0.302 |
| OLS | | <u>10917.502</u> | 0.558 | 0.487 | 2.604 |
| CatBoost | | 6206.29 | 0.57 | 0.495 | 1.0 |
| ARIMA | | <u>17727.489</u> | <u>0.278</u> | <u>0.238</u> | <u>0.593</u> |
| GPR | 12 | 19160.008 | 0.377 | 0.322 | 0.645 |
| OLS | | 13849.332 | 0.518 | 0.46 | 2.696 |
| CatBoost | | 18604.156 | 0.57 | 0.495 | 0.999 |
| ARIMA | | <u>14781.831</u> | <u>0.405</u> | <u>0.351</u> | <u>0.801</u> |
| GPR | 18 | 20955.192 | 0.074 | 0.061 | 0.707 |
| OLS | | 21764.586 | <u>0.264</u> | <u>0.226</u> | 1.662 |
| CatBoost | | <u>21170.805</u> | 0.57 | 0.495 | 0.999 |
| ARIMA | | 29662.23 | 0.36 | 0.314 | 0.598 |
| GPR | 24 | 21493.571 | <u>0.266</u> | <u>0.239</u> | 0.423 |
| OLS | | 16362.093 | 0.184 | 0.167 | 0.824 |
| CatBoost | | 33352.452 | 0.563 | 0.489 | 0.987 |
| ARIMA | | 25524.539 | 0.313 | 0.269 | <u>0.689</u> |

Table 7: Regression and calibration metrics for base models on Dataset B. Best results are highlighted with bold font, second best results are underscored

| Model | Horizon | RMSE | RMSCE | Miscal. Area | ENCE |
|----------|---------|--------------|--------------|--------------|--------------|
| GPR | 3 | 0.015 | 0.203 | 0.171 | 0.536 |
| OLS | | 0.016 | <u>0.254</u> | 0.216 | 1.839 |
| CatBoost | | 0.019 | 0.57 | 0.495 | 226.223 |
| ARIMA | | 0.015 | 0.352 | 0.295 | <u>0.733</u> |
| GPR | 6 | 0.012 | 0.258 | 0.223 | 0.554 |
| OLS | | <u>0.013</u> | <u>0.319</u> | <u>0.268</u> | 1.279 |
| CatBoost | | 0.02 | 0.57 | 0.495 | 239.636 |
| ARIMA | | 0.017 | 0.391 | 0.335 | <u>0.785</u> |
| GPR | 12 | 0.018 | 0.135 | 0.117 | 0.319 |
| OLS | | <u>0.017</u> | <u>0.259</u> | <u>0.241</u> | 1.561 |
| CatBoost | | 0.016 | 0.57 | 0.495 | 1012.208 |
| ARIMA | | 0.022 | 0.43 | 0.378 | <u>0.831</u> |
| GPR | 18 | 0.028 | 0.072 | 0.058 | 0.376 |
| OLS | | 0.028 | 0.375 | 0.316 | 2.425 |
| CatBoost | | 0.032 | 0.57 | 0.495 | 395.901 |
| ARIMA | | 0.049 | <u>0.239</u> | <u>0.201</u> | <u>0.555</u> |
| GPR | 24 | <u>0.029</u> | 0.074 | 0.066 | 0.431 |
| OLS | | 0.028 | <u>0.384</u> | 0.35 | 1.801 |
| CatBoost | | <u>0.029</u> | 0.535 | 0.455 | 2250.228 |
| ARIMA | | 0.063 | 0.435 | 0.374 | <u>0.836</u> |

C.2 Critical difference diagrams

Let us examine additional critical difference diagrams.

In the case of OLS base model (Figures 3 and 9), we can see that MEB BS OLS and Naive BS OLS are not-significantly different in terms of Miscalibration Area. Moreover, other methods are in a clique. In terms of RMSE, there are three cliques: first clique (Naive BS OLS), second clique (MEB BS OLS, OLS, Surr I OLS, Surr I OLS) and third clique (SBB BS OLS, BSAP BS OLS). In Table 2 we can see that some methods have metric values equal or close enough to the base model (OLS).

In the case of ARIMA base model (Figures 4 and 10), we see that there are three cliques in terms of Miscalibration Area and three another cliques in terms of RMSE.

In the case of CatBoost base model (Figures 5 and 11), we see that there are three cliques in the term of Miscalibration Area and two cliques in term of RMSE.

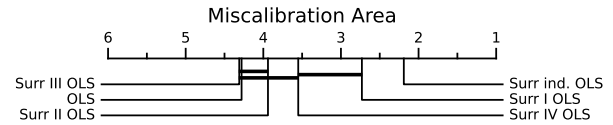


Figure 8: OLS base surrogate model comparison of Miscal. Area on Forecasting data

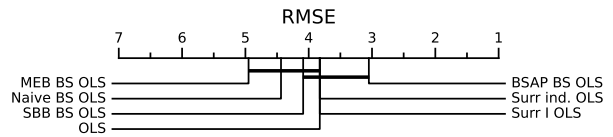


Figure 9: OLS base model comparison of RMSE on Forecasting data

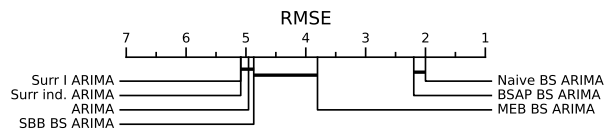


Figure 10: ARIMA base model comparison of RMSE on Forecasting data

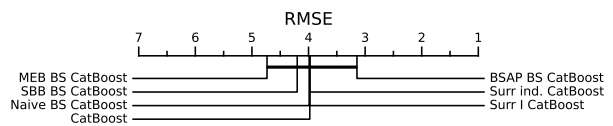


Figure 11: CatBoost base model comparison of RMSE on Forecasting data

C.3 Comparison of different surrogate approaches for different forecasting horizons

Results on Datasets A and B are visualized on Figures 12 and 13. On Dataset A, Surr Ind have metric values similar to basic approach and on Dataset B outperforms it.

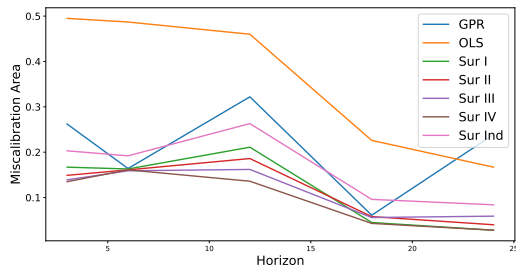


Figure 12: Performance of surrogate models on different train/test splits of Dataset A. Bigger horizon means bigger test size

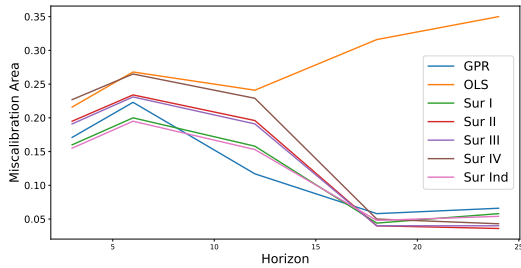


Figure 13: Performance of surrogate models on different train/test splits of Dataset B. Bigger horizon means bigger test size

C.4 Choice of hyperparameters for baseline surrogate models

In the GPR training procedure, we should define the variance value of noise in targets. During the GPR training, this parameter is tuned, but the initial value impacts the result. The noise assumption can be beneficial when we use base model predictions as targets because we incorporate the possibility of inaccuracies in base model predictions.

An expert can set the initial noise value, or we can estimate it from the training dataset. In Figure 14, we can see the dependence of the Miscalibration area on the initial noise variance size on Dataset A. Results are presented for the Surr III training type, with 20 random points added to the training dataset. The red horizontal line is the quality obtained without the usage of the noise variance. The blue curve shows test accuracy with different values of variance

assumed. The orange dot shows the quality for the variance value estimated with (3.4).

The results demonstrate that if we estimate noise variance from the training dataset, we can significantly improve the quality of the uncertainty estimation compared to the method without the noise variance selection.

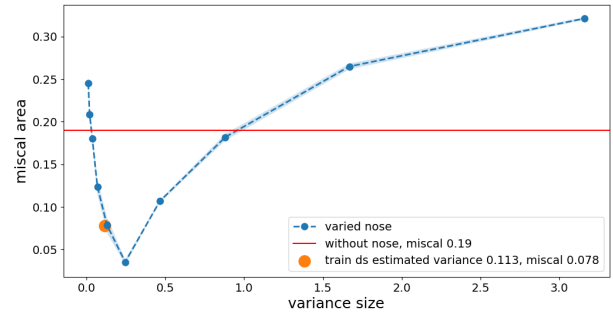


Figure 14: Influence of the noise variance on the baseline surrogate model calibration

Received 2 February 2023